Linearized waveform inversion of multicomponent blended data with polarization filters

Joseph Jennings, Biondo Biondi, Robert G. Clapp, and Shuki Ronen

ABSTRACT

We develop a new inversion scheme for linearized waveform-inversion (LWI) of blended data. We introduce polarization filters, computed from the independently modeled multicomponent data, which filter the blended data at each iteration of the inversion. We compare an approach of polarization filtering based on the Singular Value Decomposition (SVD) to our own new approach in which we extend the application of prediction-error filtering (PEF) to multicomponent data. We show that estimating PEFs using all data components provides the best deblended data which should provide much better imaging during the LWI process.

INTRODUCTION

The most difficult challenge in the direct imaging of simultaneous-source blended data is the mitigation of the artifacts that appear in the image due to cross-terms (Jiang et al., 2010). These artifacts are well understood especially in the context of LWI (least-squares migration) of phase-encoded data. While imaging of blended data is in fact quite similar to imaging of phase-encoded data, the two problems should be treated differently. This is due to the fact that with blended field data, we have a fixed encoding which cannot be changed from iteration to iteration. Changing the encoding function at each iteration, also known as dynamic phase-encoding, proves to be very useful in LWI of phase-encoded data (Boonyasiriwat et al., 2010).

While more work has been done on mitigating artifacts in phase-encoded imaging, there has been progress towards removing artifacts in imaging of blended data. In some of the earlier work, Tang et al. (2009) mitigated the artifacts with a horizontal Laplacian by adding a regularization term to the LWI objective function. Dai et al. (2011) proposed to use a deblurring filter in order to precondition the inversion and therefore achieving faster convergence. Lastly and also in the direction of regularizing the inversion, Xue et al. (2014) approached the problem by adding a shaping regularization term to the objective function.

Like the aforementioned work, we also propose to use a filter in order to mitigate the cross-term artifacts. But unlike the other approaches and following the work of Jennings and Ronen (2016), we compute our filter from the horizontal components of

multicomponent data (e.g. ocean-bottom node). Because the horizontal components have a directional dependence (as opposed to hydrophones which only measure pressure, a scalar quantity), we can know *a priori* the directionality of the source. We can estimate filters to separate the blended data based on the direction. These directional filters are known as polarization filters that are commonly used in multicomponent signal and noise separation. At each iteration of the LWI process, we estimate these polarization filters on the independently modeled shots, which serve as proxies to the deblended data. We then propose to apply these polarization filters to the blended data each each iteration of the LWI.

In this report, we first describe a new objective function that incorporates polarization filters into the LWI algorithm. We then compare two multicomponent filters, one from SVD and the other based on the theory of multidimensional non-stationary linear prediction (prediction-error filters or PEFs). We show that estimating the PEF on all components at the same time leads to better deblending results.

THEORY

Linearized blended modeling and data

For the purposes of simplified analysis, we represent a single shot gather observed in recorded seismic data by the following linear operation:

$$\mathbf{L}_i\mathbf{m} = \mathbf{d}_i, \tag{1}$$

where $\mathbf{L}_i = \mathbf{L}(\mathbf{b}, \mathbf{x}_i)$ is the linearized wave-equation (Born) modeling operator for a specific background velocity model $\mathbf{b}$ and a source location $\mathbf{x}_i$. As $\mathbf{L}$ is the linearized modeling operator, then the model vector $\mathbf{m}$ represents the reflectivity and $\mathbf{d}_i$ represents the ith shot gather of a seismic survey. With this representation of a single shot gather, we can then form a column vector of linear operators $\mathbf{L}_i$ to represent n shots and recorded data in a single seismic survey as:

$$\begin{bmatrix} \mathbf{L}_1 \\ \mathbf{L}_2 \\ \vdots \\ \mathbf{L}_n \end{bmatrix} \mathbf{m} = \begin{bmatrix} \mathbf{d}_1 \\ \mathbf{d}_2 \\ \vdots \\ \mathbf{d}_n \end{bmatrix},$$

$$\mathbf{L}\mathbf{m} = \mathbf{d}. \tag{2}$$

In order to express linearized blended modeling, we introduce the blending operator $\mathbf{\Gamma}$. This operator is linear and its primary function is to describe the blending of the data performed during the acquisition. In matrix form, it can be written as a rectangular matrix with many more columns than rows ($n > m$) where the number of rows (m) represents the extent of blending and the number of columns (n) is determined by

the number of shots. A generic form of $\mathbf{\Gamma}$ can be written as:

$$\mathbf{\Gamma} = \begin{bmatrix} \mathbf{G} & \mathbf{G} & \dots & \mathbf{0} & \mathbf{0} & \mathbf{0} & \dots & \dots & \dots & \dots & \dots & \dots \\ \mathbf{0} & \mathbf{0} & \dots & \mathbf{G} & \mathbf{G} & \mathbf{G} & \dots & \mathbf{0} & \mathbf{0} & \dots & \dots & \dots \\ \vdots & \vdots & \vdots & \dots & \dots & \dots & \dots & \mathbf{G} & \mathbf{G} & \dots & \mathbf{0} & \mathbf{0} \\ \mathbf{0} & \dots & \dots & \dots & \dots & \dots & \dots & \dots & \dots & \dots & \mathbf{G} & \mathbf{G} \end{bmatrix}_{m \times n},$$

where $\mathbf{G}$ is a phase-shift operator. For ease of notation, we use the same phase-shift operator ($\mathbf{G}$) for all shots but in general, the phase-shifts will vary from shot to shot. Applying $\mathbf{\Gamma}$ to equation 2 we arrive at an expression for modeling blended data:

$$\begin{aligned} \mathbf{\Gamma L m} &= \mathbf{\Gamma d}, \\ \widetilde{\mathbf{L}}\mathbf{m} &= \widetilde{\mathbf{d}}, \end{aligned} \tag{3}$$

where $\widetilde{\mathbf{L}}$ and $\widetilde{\mathbf{d}}$ are the linearized blended modeling operator and data respectively.

LWI of blended data

With our previously-defined blended modeling operator and data, we can write the objective function for LWI of blended data as:

$$J(\mathbf{m}) = \frac{1}{2}||\widetilde{\mathbf{L}}\mathbf{m} - \widetilde{\mathbf{d}}||_2^2. \tag{4}$$

Differentiating with respect to the model parameters we can express the gradient of equation 4 as:

$$\nabla J(\mathbf{m}) = \underbrace{\sum_{i=1}^{n} \mathbf{L}_i^* \mathbf{r}_i}_{\text{conventional}} + \underbrace{\sum_{j \neq i}^{n} \sum_{i=1}^{n} \mathbf{L}_j^* \mathbf{r}_i}_{\text{cross-terms}}, \tag{5}$$

where $\mathbf{r}_i$ is the data residual for the ith shot gather. As expected, at each iteration, our gradients will be contaminated with artifacts, seriously affecting the convergence of our LWI. These artifacts, also known as cross-talk, are due to the cross correlation of source-side Green's functions between different sources and the relative time delay between sources (Jiang et al., 2010). To suppress these artifacts, we propose to apply polarization filters estimated from the independently modeled data and applied to the to multicomponent blended data $\widetilde{\mathbf{d}}$ at each iteration resulting in an approximate deblended data. This process will be performed at each iteration resulting in iterative imaging with minimal cross-talk during the LWI process.

LWI of blended multicomponent data with polarization filters

As sources will have different azimuths in simultaneous source surveys, the recorded multicomponent data will be polarized differently providing information on the directionality of the source. Of course we can only be certain of the polarization of the

direct arrival and not of the reflections and other recorded events. To ensure that we can accurately estimate the polarization for each source, we estimate these polarization filters on independently modeled data. The independently modeled shots can be thought of as proxy data on which we estimate these polarization filters. To incorporate the use of multicomponent data and polarization filters into LWI, we propose the following objective function:

$$J(\mathbf{m}) = \frac{1}{2}||\mathbf{Lm} - \mathbf{d_p}||_2^2, \tag{6}$$

where $\mathbf{L}$ models multicomponent data (e.g. linearized elastic wave-equation operator), and $\mathbf{d_p}$ is the multicomponent data, approximately deblended via polarization filtering. Note the absence of the tilde on the linearized modeling operator. This indicates that during the LWI process, each shot will be modeled independently allowing for the computation of polarization filters on proxy shots at each iteration. In terms of the blended data, we can write the computation of $\mathbf{d_p}$ as:

$$\mathbf{d_p} = \mathbf{P}(\tilde{\mathbf{d}}) \approx \mathbf{d} \tag{7}$$

where $\mathbf{P}$, is a filtering operation that is either linear or non-linear in the blended data and utilizes the polarization in order separate one shot from another. In the remainder of this report, we describe two possible choices for $\mathbf{P}$, one based on a more traditional polarization filtering approach that utilizes the Singular Value Decomposition (SVD) of the data matrix, and the other, a new method, in which we extend the estimation of non-stationary multidimensional prediction error-filters (PEFs) to multicomponent data.

COMPARISON OF FILTERING APPROACHES

An SVD-based approach

Theory

Filtering of multicomponent data via eigendecompositions was first developed in the earthquake seismology community in order to remove elliptically polarized events from the data (e.g. surface waves) as well as to obtain an estimate of the direction-of-arrival of the earthquake source (Flinn, 1965). A key step in each of these methods is the computation of what are known as the polarization vectors (Vidale, 1986) of the data which can then be used to provide an estimate of the polarization at each point in the dataset. While the computation of these polarization vectors has been extended into other domains that are more suited for capturing non-stationary information (Barak, 2017), we only describe a time-domain implementation.

To compute the polarization vectors of our data we first construct a $nt \times nc$ size matrix where nt is length of a time window to be placed on the data and nc is the

number components we wish to analyze at a time. If we consider the case in which we only have two components (e.g. the horizontal geophone components), then we may write our data matrix $\mathbf{D}$ as:

$$\mathbf{D} = \left[\begin{array}{cc} \mathbf{y} & \mathbf{x} \end{array} \right],$$

where $\mathbf{y}$ and $\mathbf{x}$ are two column vectors of length nt that contain the data measured on the Y and X components respectively. If we then perform a reduced-SVD on this data matrix, we can write out the decomposed matrix as:

$$\mathbf{D} = \mathbf{U}\mathbf{\Sigma}\mathbf{V}^T = \mathbf{U} \left[\begin{array}{cc} \sigma_1 & 0 \\ 0 & \sigma_2 \end{array} \right] \left[\begin{array}{c} \mathbf{v}_1^T \\ \mathbf{v}_2^T \end{array} \right],$$

where $\mathbf{U}$ is a $nt \times 2$ matrix that contains the left singular vectors, σ_1 and σ_2 are the singular values and $\mathbf{v_1}$ and $\mathbf{v_2}$ are the right singular vectors, or our orthornormal polarization vectors. As in an SVD, the first singular value (σ_1) is defined to be the largest singular value, then $\mathbf{v_1}$, its associated polarization vector, will describe the dominant polarization on that data trace for the chosen time window. To develop a better understanding of why the right singular vectors of the SVD of the data matrix give an estimate of the polarization in the data, it is helpful to recall that the right, scaled singular vectors that result from an SVD of a 2×2 matrix will give the principal axes of an ellipse (Trefethen and Bau III, 1997). Notice also that in its simplest form, the hodogram of a multicomponent seismogram can be described by an ellipse and the largest principal axis of the hodogram ellipse describes the dominant polarization direction of the data. Therefore, the right singular vectors of a data matrix $\mathbf{D}$ will provide an estimate of the maximum direction of polarization in the data. A visual example of this for two phase-shifted, monochromatic signals is shown in Figure 1. For a more rigorous explanation on the connection between polarization in multicomponent seismic data and the right singular vectors obtained via SVD we refer the reader to Montalbetti and Kanasewich (1970) and Jackson et al. (1991).

Application to filtering multicomponent blended data

As these polarization vectors give an estimate of the direction of the data, we can use them to design filters that will remove parts of the data that have an undesired direction. In the context of simultaneous-source acquisition, when sources have different azimuths their direct arrivals will be polarized differently and therefore can be suppressed with a polarization filter. In addition, depending on the geometry of the subsurface, we can also remove other events that originate from that source if they have different polarization than events coming from the other shot.

Figure 2 shows the acoustic wavefields and the recorded particle velocities (v_y, v_x) as a result of two shots. The blue line indicates the receiver locations. One shot was positioned cross-line to receiver positions (Figure 2a) and another directly inline with the receiver positions (Figure 2b). Because of these shot locations, the data are highly polarized in the Y and X directions as is evident by the shot gathers of

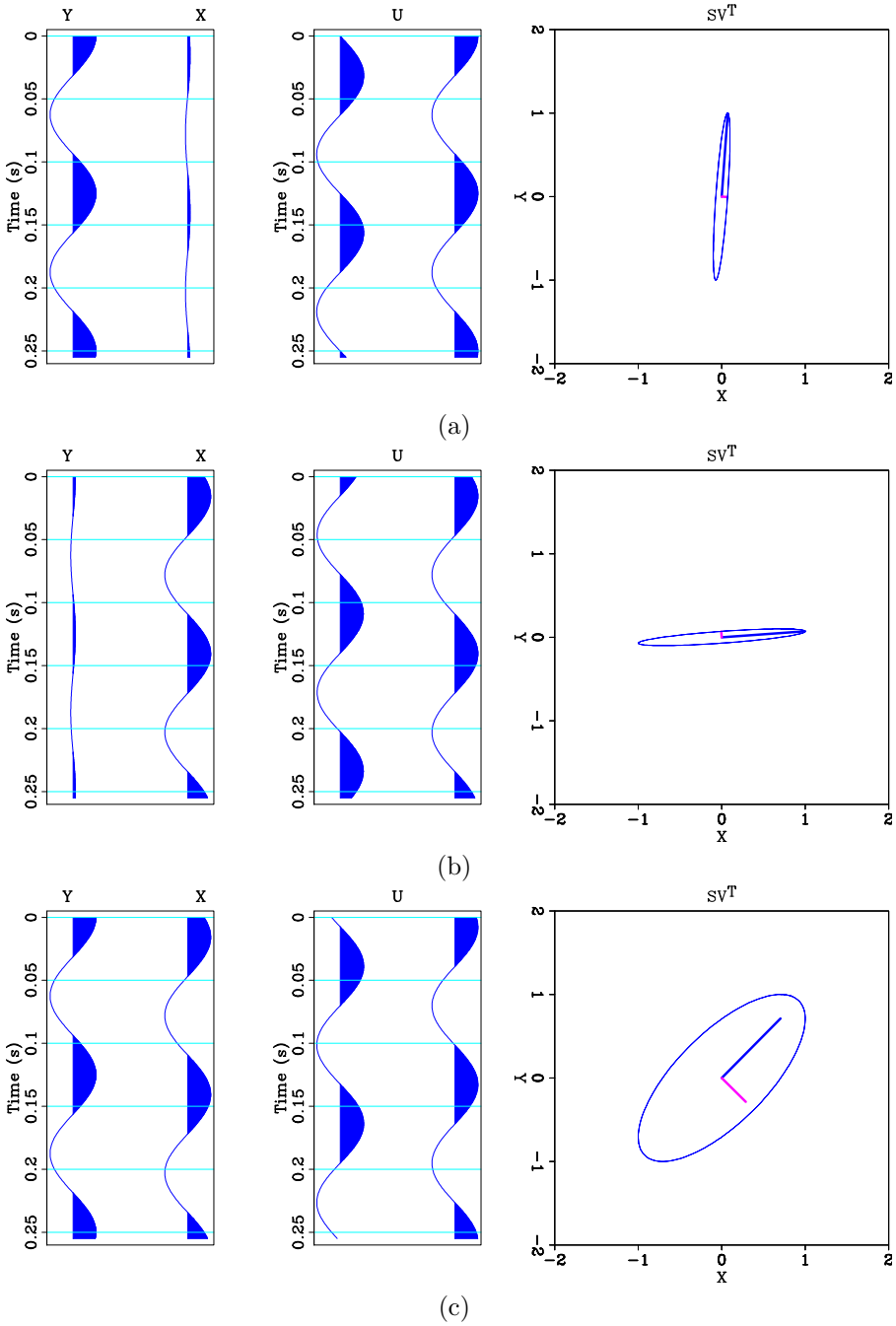

Figure 1: Three simple examples of polarization analysis via SVD. The left wiggle plot of each subpanel shows $\mathbf{D} = [\mathbf{y} \quad \mathbf{x}]$. The right wiggle plot in each panel shows the computed $\mathbf{U}$ of the SVD. The rightmost plot shows the scaled singular vectors $\mathbf{\Sigma V}^T$ overlain on the hodogram. Panel (a) shows an example in which the majority of the energy is on the Y component. This is evident by the hodogram and the right singular vector that point in the Y direction. Panel (b) shows now a similar situation but now the majority of the energy is located on the X component. Panel (c) shows the polarization analysis now of a multicomponent signal of mixed polarization. Note that the singular vectors are in fact the principal axes of the hodogram ellipse (as is defined by the SVD) thus providing the polarization information. [**ER**]

the horizontal components (Figures 2c-2f). In another experiment, these two shots occurred with a much shorter shot interval resulting in blended data. The recorded blended particle velocities are shown in Figures 3a-3b. Because these blended data are highly polarized, it provides a simple example in which we can use polarization filters to separate the two arrivals.

In order to design polarization filters for these blended data and blended data in general, let us first examine the SVD of the data matrices of the independently modeled shots $\mathbf{D}_1$ and $\mathbf{D}_2$ (Figure 2):

$$\mathbf{D_1} = \left[\begin{array}{cc} \mathbf{y}_1 & \mathbf{x}_1 \end{array} \right] = \mathbf{U_1 \Sigma_1} \left[\begin{array}{c} \mathbf{v}_{11}^T \\ \mathbf{v}_{12}^T \end{array} \right], \mathbf{D_2} = \left[\begin{array}{cc} \mathbf{y}_2 & \mathbf{x}_2 \end{array} \right] = \mathbf{U_2 \Sigma_2} \left[\begin{array}{c} \mathbf{v}_{21}^T \\ \mathbf{v}_{22}^T \end{array} \right],$$

where $\mathbf{v}_{ij}$ indicates the ith shot for the jth polarization vector. When the shots have different azimuths, then the polarization vectors of each shot $(\mathbf{v}_{11}, \mathbf{v}_{12})$ and $(\mathbf{v}_{21}, \mathbf{v}_{22})$ will point in different directions. In fact, when the two shots have orthogonal azimuths, then their polarization vectors will also be orthogonal. For the data shown in Figure 2, we can compute the polarization vectors for each and every time sample. If we then take both components of the largest polarization vector and plot them for each and very time sample of the gathers shown in Figure 2, we can visualize the strength of the Y and X polarization at each point in the data. Figure 4 shows result of carrying-out this process. It is clear that for the majority of the points in the gather, the polarization vectors are indeed orthogonal.

Using the fact that sources with different azimuths will lead to different polarization vectors, we can construct filters based on the inner-product of the independently modeled polarization vectors with the polarization vectors of the blended data. In places where the blended data are polarized in the same direction as one of the shots, the inner-product will be large and in places where they are nearly orthogonal, the inner-product will be small. From this, we can arrive at an expression for the polarization filter coefficients. First, we compute the polarization vectors of the blended data:

$$\widetilde{\mathbf{D}} = \widetilde{\mathbf{U}} \widetilde{\mathbf{\Sigma}} \left[\begin{array}{c} \widetilde{\mathbf{v}_1}^T \\ \widetilde{\mathbf{v}_2}^T \end{array} \right].$$

Then computing the inner-products of the largest polarization vectors of the independently modeled data with the largest polarization vector of the blended data, we can construct a 2×1 vector of weights that can be applied to each component of the blended data for each time sample:

$$f_1 = \mathbf{v}_{11}^T \widetilde{\mathbf{v}_1}, \quad f_2 = \mathbf{v}_{21}^T \widetilde{\mathbf{v}_1},$$

$$\left[\begin{array}{c} v_{y_1} \\ v_{y_2} \end{array} \right]_{it} = \left[\begin{array}{c} |f_1|^n \\ |f_2|^n \end{array} \right]_{it} \widetilde{v_{y_{it}}},$$

$$\left[\begin{array}{c} v_{x_1} \\ v_{x_2} \end{array} \right]_{it} = \left[\begin{array}{c} |f_1|^n \\ |f_2|^n \end{array} \right]_{it} \widetilde{v_{x_{it}}},$$

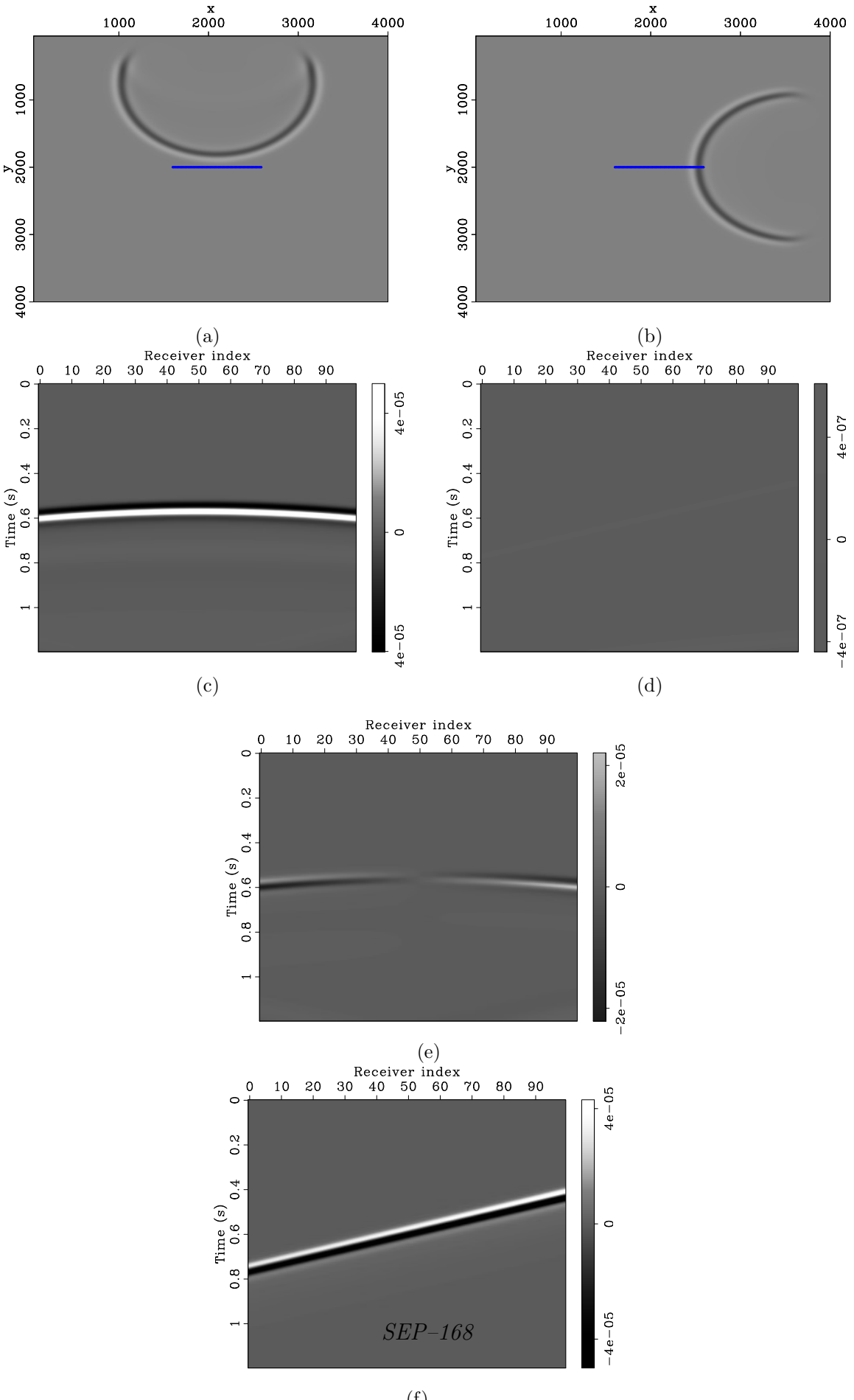
x
1000
2000
3000
4000
y
1000
2000
3000
4000
(a)
(b)
Receiver index
0 10 20 30 40 50 60 70 80 90
Time (s)
0 0.2 0.4 0.6 0.8 1
4e−05
0
−4e−05
(c)
4e−07
0
−4e−07
(d)
2e−05
−2e−05
(e)
SEP–168
(f)

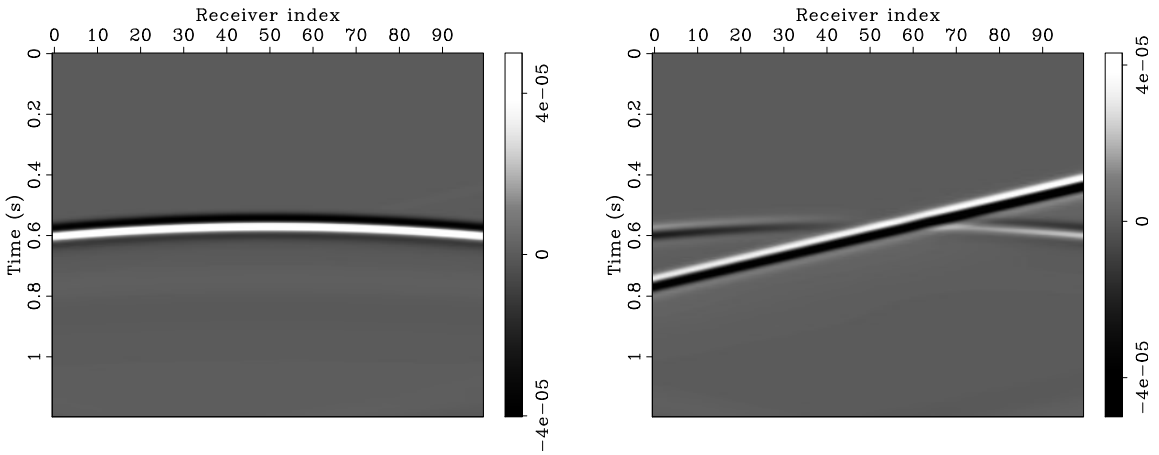

(a) (b)

Figure 3: Multicomponent blended data. (a) Y component of particle velocity. (b) X component of particle velocity. Note that the energy from shot two was not recorded on the Y component because it was completely polarized in the X direction (Figure 2e). [**ER**]

where v_{y_1}, v_{y_2}, v_{x_1} and v_{x_2} are the deblended Y and X components of the particle velocity of shot one and shot two, f_1 and f_2 are the two weights and n is an integer to increase the strength of the filtering. We apply this filtering scheme to blended data shown in Figure 3 and obtain the approximately deblended data shown in Figure 5.

Multicomponent PEFs

In addition to the SVD filter, we also investigated the use of non-stationary PEFs in order to approximately deblend the data. Because PEFs act as annihilation filters when the prediction-error is small, they are well-suited for signal and noise separation which include deblending applications (Spitz et al., 2008). Because we desire that the PEF use the polarization information to aid in the prediction, we estimate PEFs on all of the components at the same time. To verify our implementation of multicomponent PEF estimation, we compare the PEF estimated on all components simultaneously with PEFs estimated on the components separately. For a description of the algorithm we use for estimating non-stationary PEFs, we refer to Ruan et al. (2015).

Theory

Again, starting from the independently modeled data we can estimate non-stationary PEFs on the independently modeled shots, which serve as annihilators for each shot.

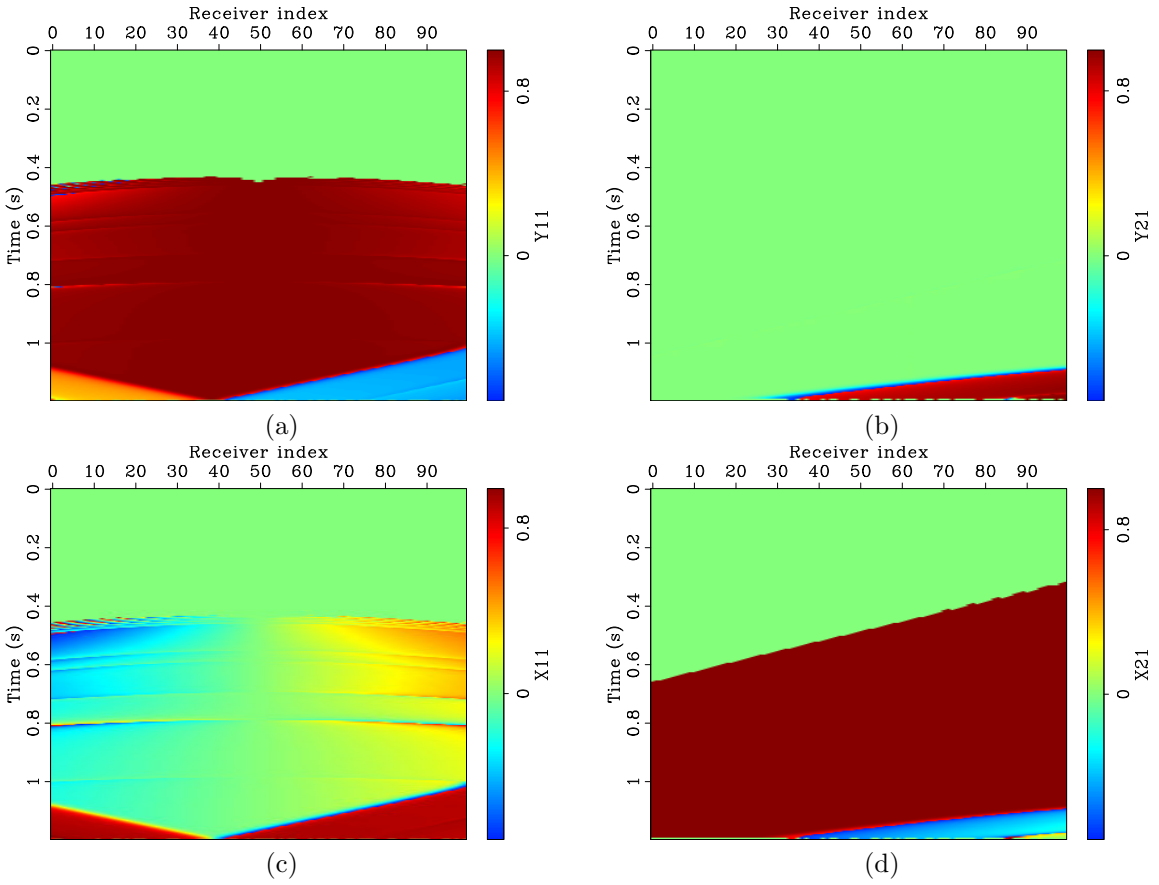

Figure 4: Y and X components of the largest polarization vector of shots one and two. (a) Y component of the strongest polarization vector of shot one. (b) Y component of the largest polarization vector of shot two. (c) X component of the largest polarization vector of shot one. (d) X component of the largest polarization vector of shot two. Comparing the magnitudes of each of the components of the vectors, it is clear that at almost every point in the data the vectors $\mathbf{v}_{11}$ and $\mathbf{v}_{21}$ are nearly orthogonal. [**ER**]

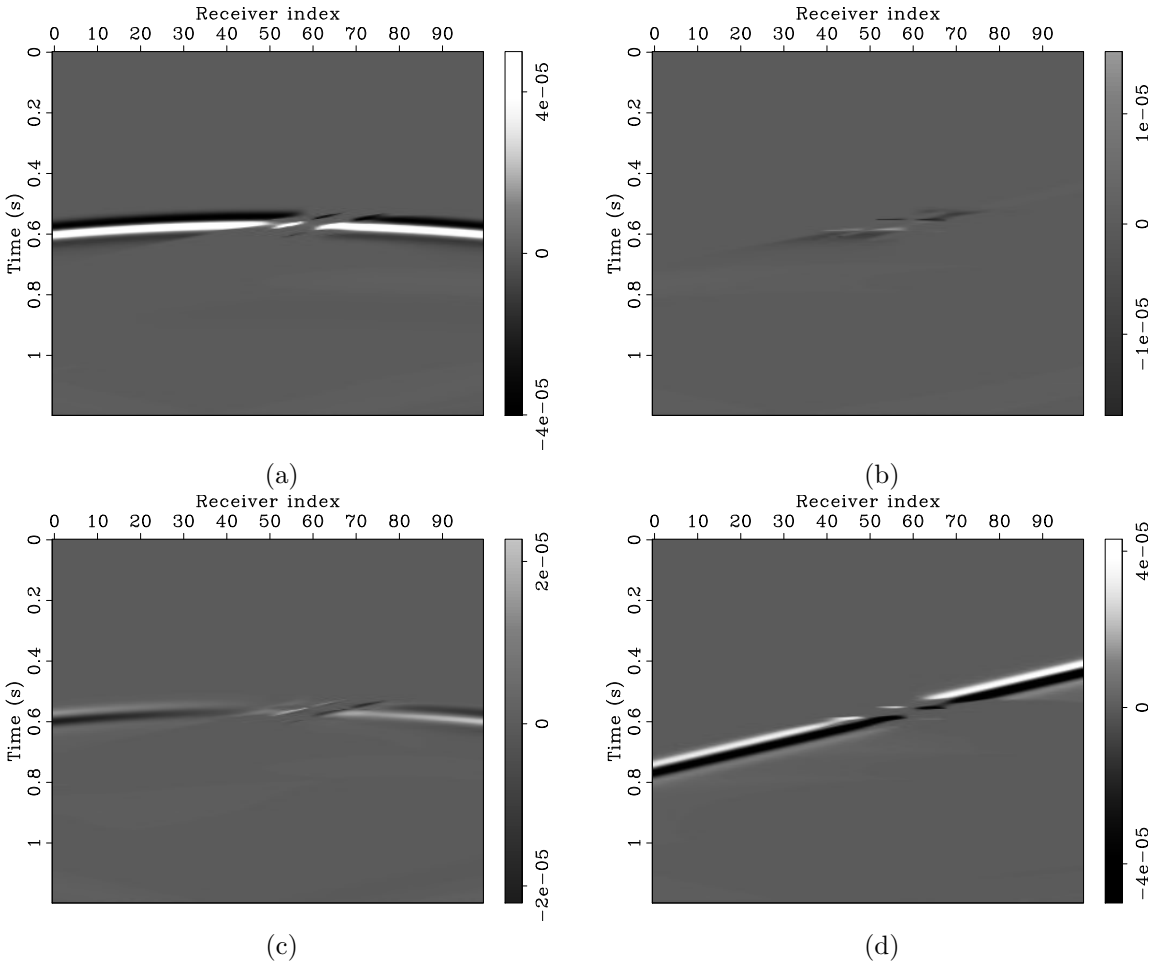

Figure 5: Approximately deblended data via the SVD-based polarization filtering. (a) Deblended Y component of shot one. (b) Deblended Y component of shot two. (c) Deblended X component of shot one. (d) Deblended X component of shot two. It appears that the filtering algorithm did a reasonable job at what it was designed to do: remove events that are not polarized in the direction of the independently modeled shots. Note that the method performs poorly when the two events overlap. [**ER**]

To do this, we estimate the PEFs $\mathbf{f}_1$ and $\mathbf{f}_2$ from the following system of regressions:

$$\overline{\mathbf{D}}_1\mathbf{f}_1 \approx \mathbf{0}, \tag{8}$$

$$\overline{\mathbf{D}}_2\mathbf{f}_2 \approx \mathbf{0}, \tag{9}$$

where $\overline{\mathbf{D}}_1$ and $\overline{\mathbf{D}}_2$ are the data from shot gather one and two respectively formed into convolution matrices. Upon solving for these filters, we can then use them to separate shots one and two by minimizing the following objective function:

$$J(\mathbf{d}_1, \mathbf{d}_2) = \frac{1}{2}||\mathbf{d}_1 + \mathbf{d}_2 - \widetilde{\mathbf{d}}||_2^2 + \frac{1}{2}||\overline{\mathbf{F}}_1(\mathbf{d}_2 - \widetilde{\mathbf{d}})||_2^2 + \frac{1}{2}||\overline{\mathbf{F}}_2(\mathbf{d}_1 - \widetilde{\mathbf{d}})||_2^2, \tag{10}$$

where $\mathbf{d}_1$ and $\mathbf{d}_2$ are the data from shots one and two respectively now written as column vectors and $\overline{\mathbf{F}}_1$ and $\overline{\mathbf{F}}_2$ are the PEFs estimated from expressions 8 and 9 now expressed as convolutional operators. The first term of this objective function is the familiar deblending objective that requires that the sum of the estimated shots be equal to the blended data. The other two terms act to enforce the separation of the two shots (Abma, 1995).

Single vs. multicomponent PEFs

Although the above algorithm may provide a manner in which to deblend the data at each iteration of the LWI process, we need to extend the current use of single component PEFs, to multicomponent data, in which the PEF is estimated simultaneously using all data components. In doing so, we expect that the PEF has the possibility of incorporating polarization information into its coefficients that could annihilate unwanted noise not only by a non-stationary temporal or spatial signature, but also based on the direction from which it originated. In doing so, these multicomponent PEFs become powerful tools not only for separating multicomponent blended data, but also for other multicomponent signal processing applications typical in land and ocean-bottom node settings. While all of the theory has yet to be developed, we currently extend the 2D single component PEF along the component axis. This then makes the 2D single component PEF now a 3D PEF estimated on 2D multicomponent data. A typical single component PEF is shown in Figure 6a and the new multicomponent PEF is shown in Figure 6b.

Application to filtering multicomponent blended data

With the data shown in Figure 3 as our $\widetilde{\mathbf{d}}$, we minimized the objective function in equation 10 to compute the approximately deblended data. The results of minimizing expression 10 using single component PEFs are shown in Figure 7 and the results using multicomponent PEFs are shown in Figure 8. Both inversion results completely recover the two shots on each component and therefore would provide a good $\mathbf{d}_p$ during the LWI process.

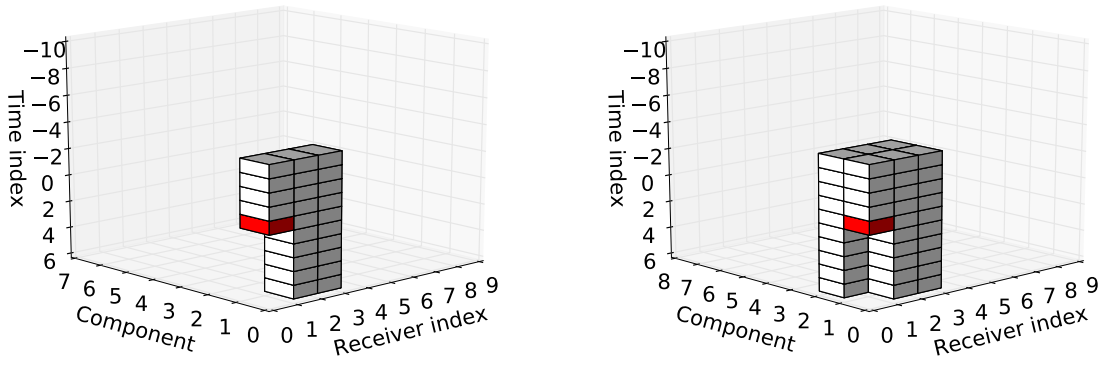

(a) (b)

Figure 6: (a) 2D Single component and (b) 2D multicomponent PEF design. The red sample indicates the location of the zero lag (where the prediction will be made). In order to use the additional direction information provided by the multicomponent data, we extend the current 2D single component PEF along the component axis, to create the multicomponent PEF. In addition to using previous temporal samples and the two spatial lags, the multicomponent PEF will use the spatial lags as well as previous and future samples from the other component to make predictions on the current component. [**ER**]

DISCUSSION

Single and multicomponent PEF comparison

While the single and multicomponent PEFs provide similar filtering results, we find differences when we examine the model updates at each iteration. Figure 9 shows the comparison of the model updates of the X component of shot one after 60 iterations of both the single and multicomponent PEF approaches. Observing the model residual plot shown in Figure 9c, it is readily apparent that the deblending using the multicomponent PEF greatly outperforms the deblending with the single component PEF. Moreover, examining the deblending misfit at each iteration shown in Figure 9d, we see that using the multicomponent PEF also provides an overall better fit to the data. While we do not yet understand all of the reasons for why this occurs, a simple explanation is that extending the PEF along the component axis allows the filter to better distinguish the signal and noise (Abma, 1995). This is because in addition to the temporal and spatial axes, we have the component axis. It is also possible that the additional information provided on the component axis that the PEF uses for prediction is in fact polarization information thus making these multicomponent PEFs polarization filters. We are currently in the process of running more numerical experiments to gain a better intuition for these multicomponent PEFs.

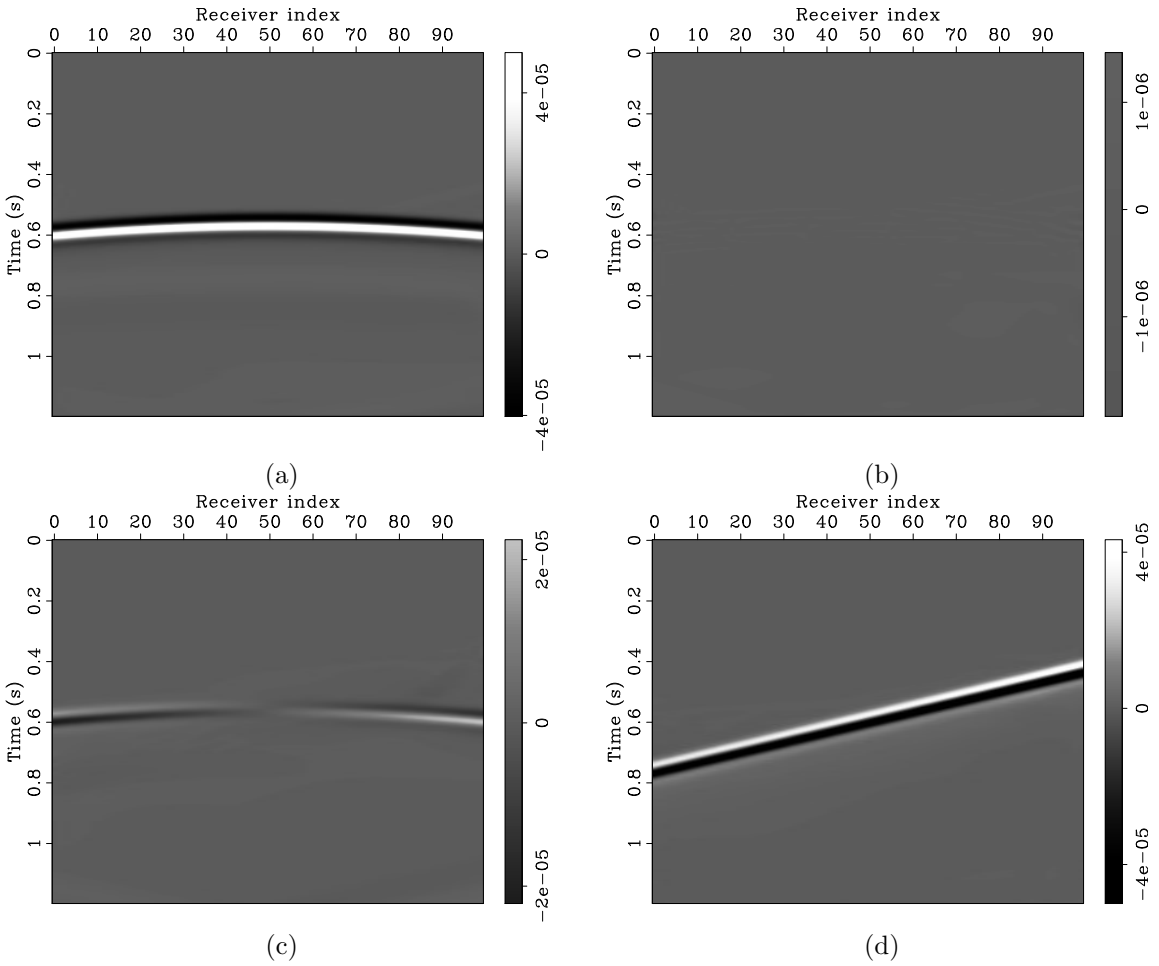

Figure 7: Approximately deblended data via minimizing equation 10 using single component PEFs (Figure 6a). (a) Deblended Y component of shot one. (b) Deblended Y component of shot two. (c) Deblended X component of shot one. (d) Deblended X component of shot two. It appears that the inversion completely recovered both shots on each of the components. [**ER**]

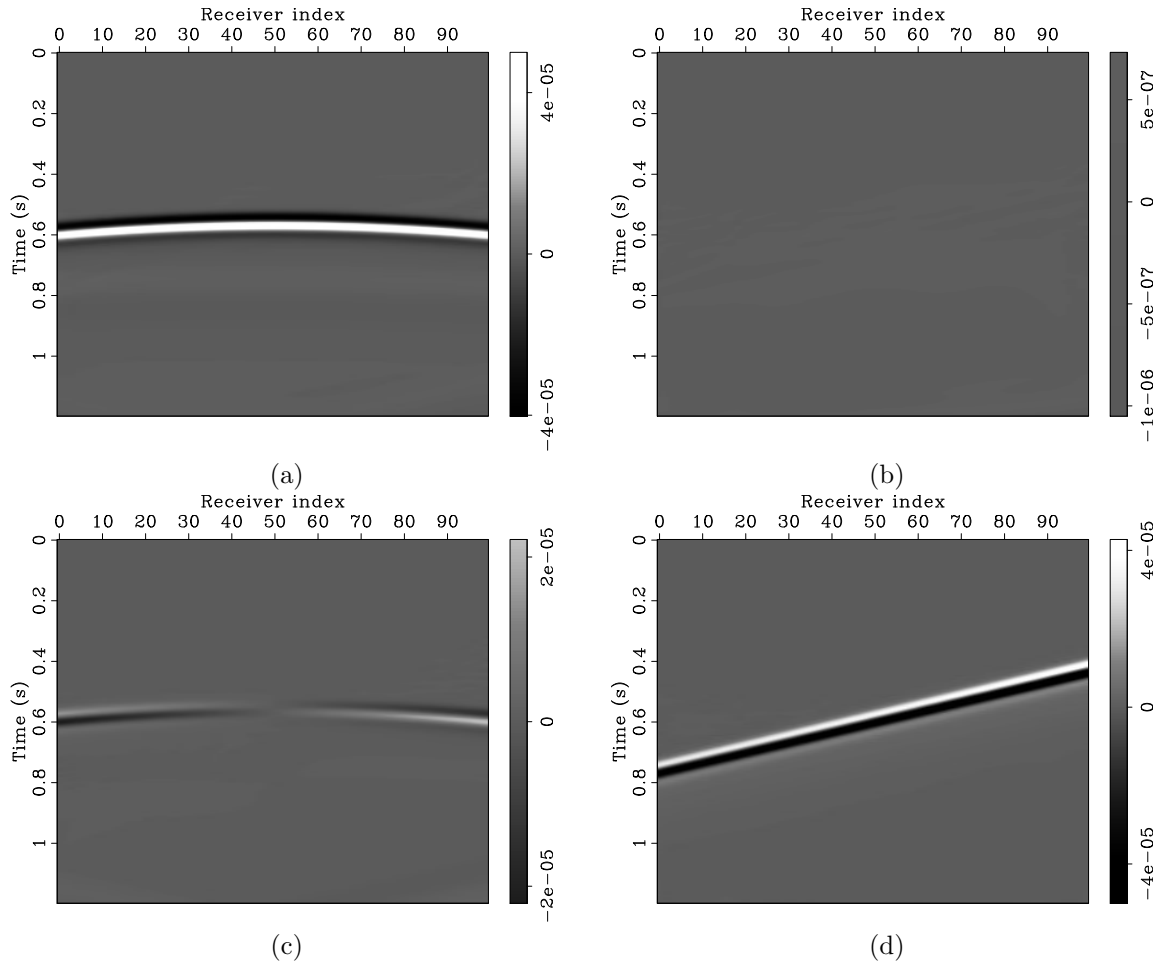

Figure 8: Approximately deblended data via minimizing equation 10 using multicomponent PEFs (Figure 6b). (a) Deblended Y component of shot one. (b) Deblended Y component of shot two. (c) Deblended X component of shot one. (d) Deblended X component of shot two. The results are quite similar to the single component results and completely recovered both shots on each of the components. [**ER**]

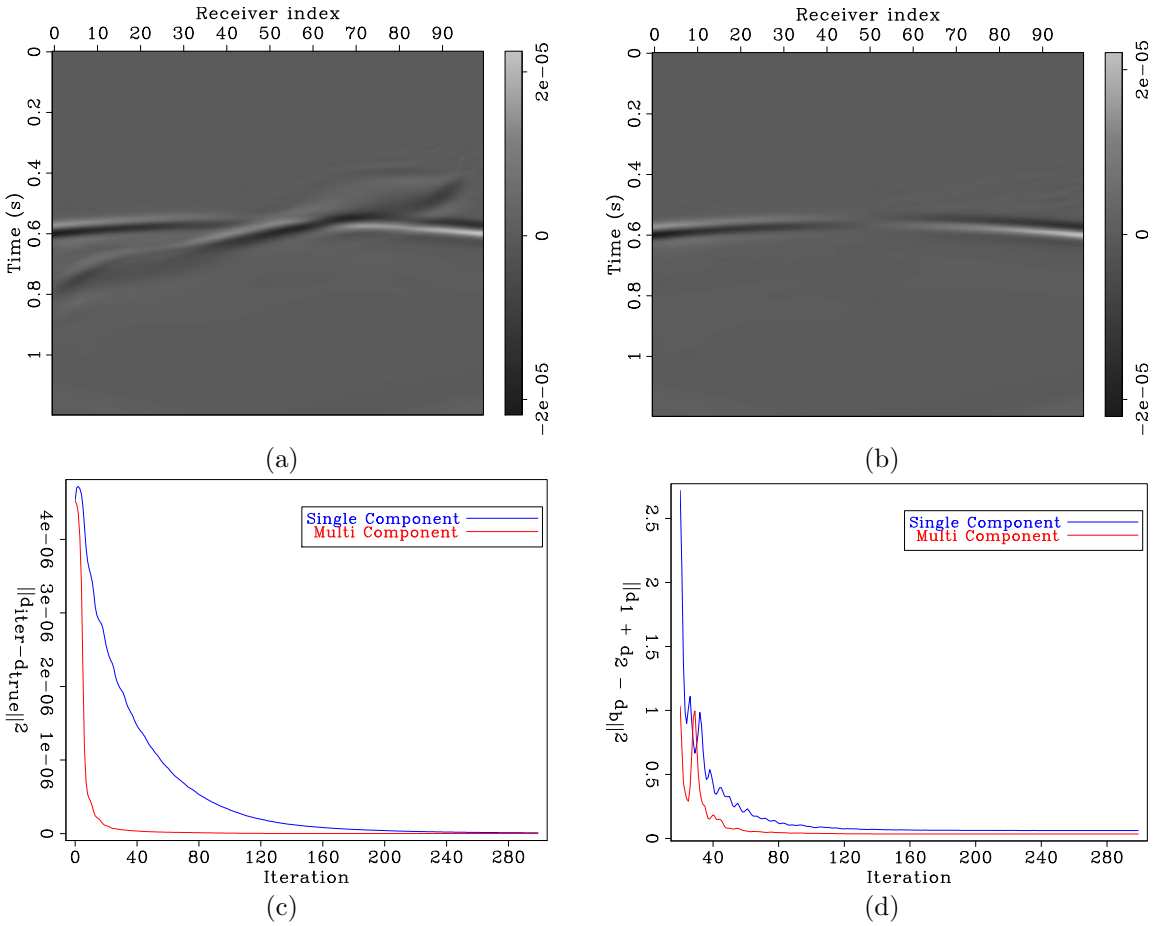

Figure 9: (a) The updated X component of shot one after 60 iterations of minimizing the objective function in equation 10 using a single component PEF. (b) The updated X component of shot one after 60 iterations of the same inversion, but using the multicomponent PEF. (c) The model residual of the single component (blue) and the multicomponent (red) PEF inversions. (d) The deblending data residual (first term in equation 10) of the single component (blue) and multicomponent (red) PEF inversions. After 60 iterations, while the single component PEF result still has a significant amount of noise from the other shot, the multicomponent appears to have nearly recovered the signal. [**ER**]

SVD and multicomponent PEF comparison

Comparing the results of the two multicomponent filters (SVD vs multicomponent PEF) shown in Figures 5 and 8, it is apparent that the PEF-based approach provided much better results. While it is possible to extend the SVD-based approach beyond a 1D diagonal weighting operator (Schimmel and Gallart, 2003; Paulus and Mars, 2006) that would lead to better filtering results, we prefer the PEF approach as it more naturally extends to a convolutional filter (linear operator) formulation that can used for multidimensional signal and noise separation. Additionally, the PEF-based approach is entirely linear in the data, whereas the SVD introduces additional non-linearity into our new LWI process. In spite of the results obtained using the multicomponent PEF, we are still uncertain of how much of the directional information it uses in the signal and noise separation, while the SVD-based filtering is designed to remove noise that has a specific polarization. While there do exist parallels between the SVD-based filter and the multicomponent PEF, much more research has yet to be done on this topic.

CONCLUSION

We have presented a new algorithm that has the potential to provide better images resulting from LWI of simultaneous-source blended data. In addition to the traditional LWI of blended data, this algorithm requires that at each iteration the shots be modeled independently and that polarization filters be estimated on these proxy shots. These polarization filters will be later applied on the blended data providing a preconditioned data. As this occurs at each iteration, this in fact turns the linear inversion, into a non-linear inversion where the objective function changes at each iteration. We presented a potentially new polarization filter, the multicomponent PEF, that provided the best filtering results when compared to traditional SVD-based polarization filters and single component PEFs. The estimation and application of these multicomponent PEFs at each iteration of LWI can potentially reduce the cross-talk artifacts that are introduced into the gradients at each iteration of LWI therefore providing overall better convergence of LWI of blended data.

ACKNOWLEDGEMENTS

We would like to thank the sponsors of the SEP for their financial and intellectual support. Additionally, the first author would like to thank Ohad Barak for helping him through the basics of SVD-based polarization filtering.

REFERENCES

Abma, R. L., 1995, Least-squares separation of signal and noise using multidimensional filters: PhD thesis, Stanford University.

Barak, O., 2017, Seismic rotational data: Acquisiton, processing and applications: PhD thesis, Stanford University.

Boonyasiriwat, C., G. T. Schuster, et al., 2010, 3d multisource full-waveform inversion using dynamic random phase encoding: Presented at the 2010 SEG Annual Meeting.

Dai, W., X. Wang, and G. T. Schuster, 2011, Least-squares migration of multisource data with a deblurring filter: Geophysics, **76**, R135–R146.

Flinn, E., 1965, Signal analysis using rectilinearity and direction of particle motion: Proceedings of the IEEE, **53**, 1874–1876.

Jackson, G., I. Mason, and S. Greenhalgh, 1991, Principal component transforms of triaxial recordings by singular value decomposition: Geophysics, **56**, 528–533.

Jennings, J. and S. Ronen, 2016, Deblending using the radiality attribute: SEP-Report, **165**, 123–132.

Jiang, Z., R. Abma, et al., 2010, An analysis on the simultaneous imaging of simultaneous source data: Presented at the 2010 SEG Annual Meeting.

Montalbetti, J. F. and E. R. Kanasewich, 1970, Enhancement of teleseismic body phases with a polarization filter: Geophysical Journal International, **21**, 119–129.

Paulus, C. and J. I. Mars, 2006, New multicomponent filters for geophysical data processing: IEEE transactions on geoscience and remote sensing, **44**, 2260–2270.

Ruan, K., J. Jennings, E. Biondi, R. G. Clapp, et al., 2015, Industrial scale high-performance adpative filtering with PEF applications: SEP-Report, **160**, 181–192.

Schimmel, M. and J. Gallart, 2003, The use of instantaneous polarization attributes for seismic signal detection and image enhancement: Geophysical Journal International, **155**, 653–668.

Spitz, S., G. Hampson, and A. Pica, 2008, Simultaneous source separation: A prediction-subtraction approach, *in* SEG Technical Program Expanded Abstracts 2008, 2811–2815, Society of Exploration Geophysicists.

Tang, Y., B. Biondi, et al., 2009, Least-squares migration/inversion of blended data: Presented at the 2009 SEG Annual Meeting.

Trefethen, L. N. and D. Bau III, 1997, Numerical linear algebra, volume **50**: Siam.

Vidale, J. E., 1986, Complex polarization analysis of particle motion: Bulletin of the Seismological society of America, **76**, 1393–1405.

Xue, Z., Y. Chen, S. Fomel, J. Sun, et al., 2014, Imaging incomplete data and simultaneous-source data using least-squares reverse-time migration with shaping regularization: Presented at the 2014 SEG Annual Meeting.